Journal of Medicinal Chemistry

Article

pubs.acs.org/jmc

Tweaking Subtype Selectivity and Agonist Efficacy at (*S*)-2-Amino-3-(3-hydroxy-5-methyl-isoxazol-4-yl)propionic acid (AMPA) Receptors in a Small Series of BnTetAMPA Analogues

Shuang-Yan Wang,[†,‡] Younes Larsen,[†] Cristina Vara Navarrete,[†] Anders A. Jensen,[*,†] Birgitte Nielsen,[†] Ali Al-Musaed,[†] Karla Frydenvang,[†] Jette Sandholm Kastrup,[*,†] Darryl S. Pickering,[*,†] and Rasmus Prætorius Clausen[*,†]

[†]Department of Drug Design and Pharmacology, Faculty of Health and Medical Sciences, University of Copenhagen, Universitetsparken 2, DK 2100 Copenhagen, Denmark

[‡]Department of Biochemistry and Molecular Biology, Gene Engineering and Biotechnology Beijing Key Laboratory, Beijing Normal University, Beijing 100875, P. R. of China

Supporting Information

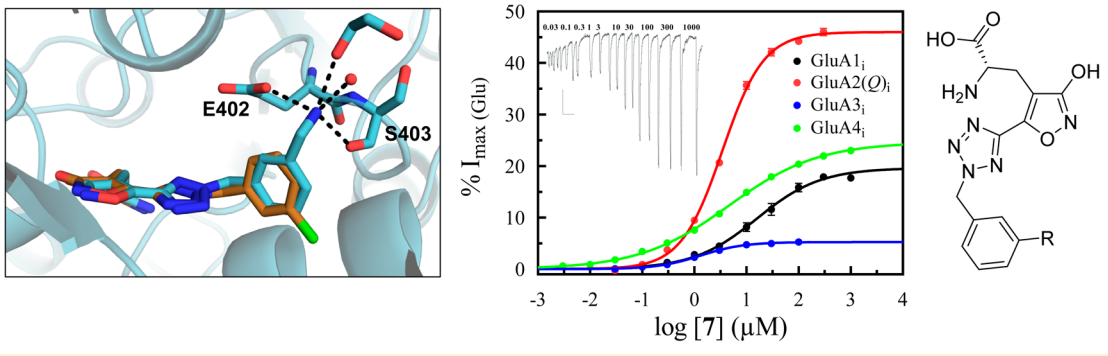

ABSTRACT: A series of analogues of the (*S*)-2-Amino-3-(3-hydroxy-5-methyl-isoxazol-4-yl)propionic acid (AMPA) receptor agonist BnTetAMPA (**5b**) were synthesized and characterized pharmacologically in radioligand binding assays at native and cloned AMPA receptors and functionally by two-electrode voltage clamp electrophysiology at the four homomeric AMPA receptors expressed in *Xenopus laevis* oocytes. The analogues **6** and **7** exhibit very different pharmacological profiles with binding affinity preference for the subtypes GluA1 and GluA3, respectively. X-ray crystal structures of three ligands (**6**, **7**, and **8**) in complex with the agonist binding domain (ABD) of GluA2 show that they induce full domain closure despite their low agonist efficacies. Trp767 in GluA2 ABD could be an important determinant for partial agonism of this compound series at AMPA receptors, since agonist efficacy also correlated with the location of the Trp767 side chain.

INTRODUCTION

(*S*)-Glutamic acid (glutamate, Glu, **1**, Chart 1) is the major excitatory neurotransmitter in the brain and has a central role for the normal functions of the brain. On the other hand, the neurotransmitter is also involved in a number of central nervous system disorders.[1] The physiological and pathophysiological effects of Glu are mediated by a highly heterogeneous receptor population comprising G-protein coupled metabotropic Glu receptors and ionotropic Glu receptors (iGluRs).[1] The iGluRs are Glu-gated cation channels that can be further divided into three major classes according to their respective activation by the agonists *N*-methyl-D-aspartic acid (NMDA), (*S*)-2-amino-3-(3-hydroxy-5-methyl-isoxazol-4-yl)propionic acid ((*S*)-AMPA, **2**), and kainic acid (kainate, KA).[2,3] The iGluRs are homo- or heteromeric assemblies of various subunits, NMDA receptors being made up of the GluN1, GluN2A−D, or GluN3A,B subunits, AMPA receptors of the GluA1−4 subunits, and KA receptors of the GluK1−5 subunits. Recent X-ray crystallographic studies of full-length AMPA and NMDA receptors have confirmed that the iGluR is a tetrameric assembly[4−8] consisting of three structural domains, the transmembrane domain forming the ion channel, an agonist binding domain (ABD), and a large N-terminal domain. Prior to these structures, a large number of structures of soluble constructs of the iGluR ABDs had disclosed important information on the molecular basis for orthosteric ligand recognition, and the mechanisms underlying activation, desensitization, and allosteric modulation of the receptors.[9] The ABD is a clamshell-like structure with two lobes closing around the agonist upon receptor activation, and the degree of receptor activation has been proposed to be closely linked to

Received: December 22, 2015

DOI: 10.1021/acs.jmedchem.5b01982
J. Med. Chem. XXXX, XXX, XXX−XXX

Chart 1. Chemical Structures of Glutamic Acid and Some Selective iGluR Agonists 1−5a,b and the New Compounds 6−11

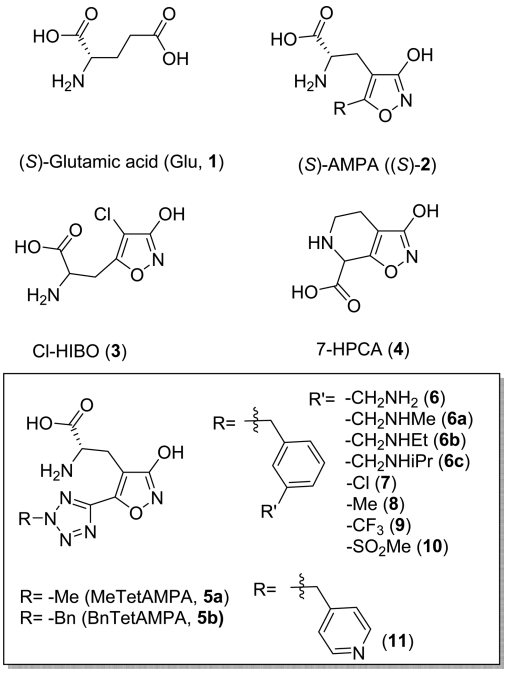

the degree of domain closure around the orthosteric ligand.[10,11] The details on how domain closure translates into channel opening are unknown, but H−D exchange NMR studies of various full and partial agonists have provided details on the dynamics of domain closure that are not observed in the X-ray crystal structures.[12−14] The studies showed that domain closure induces a number of H-bonds between the upper and lower lobes in the clamshell that are weaker for partial agonists than for full agonists and that efficacy can be correlated with the stability of these hydrogen bonds. In particular, large differences in the NMR signal from the indole N−H of Trp767 was observed for a series of substituted willardiines.[12] It is currently unknown whether the ABD X-ray structures reflect a partially activated state of the receptor or rather are slightly stabilized intermediate states in a range of different conformations in a more dynamic system. More recently, full-length X-ray crystal structures containing partial agonists have been achieved giving more insight on the activation mechanisms[7,8] but with little information on the dynamics, and as yet structures of the open channel state of GluA2 have not been reported.

The medicinal chemistry efforts in the iGluR field have resulted in the development of several agonists with selective activity at the receptors comprised of one of the three major iGluR classes, that is, the NMDA, AMPA, or KA receptors.[1] In contrast, agonists (and antagonists) discriminating between different subtypes within these three classes are very few and far between due to the high degree of sequence identity for the orthosteric sites of the respective subunits within each class. In the AMPA receptor field, the compounds **3** and **4** have been found to be selective agonists of GluA1 and GluA2 over the GluA3 and GluA4 subtypes.[15,16] A single residue in the orthosteric site of the AMPA receptors has been found to be the key molecular determinant: a tyrosine in the GluA1/2 ABD that is a phenylalanine in GluA3/4. In another series of analogues, the potent but completely nonselective AMPA receptor agonist 2-amino-3-[3-hydroxy-5-(2-methyl-2*H*-5-tetrazolyl)-4-isoxazolyl]propionic acid (MeTetAMPA, **5a**) was employed as lead structure in the development of 2-amino-3-[3-hydroxy-5-(2-benzyl-2*H*-5-tetrazolyl)-4-isoxazolyl]propionic acid (BnTetAMPA, **5b**),[17,18] which selectively activates GluA2, GluA3, and GluA4 over GluA1. This subtype preference was shown to not arise from the above-mentioned tyrosine/phenylalanine difference in the Glu binding site of the receptors but rather to be rooted in interactions of the benzyl group of BnTetAMPA with residues in a less conserved region in the proximity of the Glu binding site.[19] Trauner and co-workers recently developed **5b** into a photoswitchable AMPA receptor agonist, but the subtype selectivity profile of this compound was not established.[20,21] Furthermore, an X-ray crystal structure of **5b** in the GluA2 ABD demonstrated that **5b** induces a high degree of domain closure (21.5°) but is nevertheless a partial agonist with an efficacy of 0.83 compared with Glu.[18] There is considerable potential in subtype-selective AMPA receptor ligands as pharmacological tools for the delineation of the physiological functions governed by the respective subtypes. The interesting pharmacological properties of **5b** and the apparent importance of the side pocket adjacent to the Glu binding site targeted by the benzyl group of **5b** for subtype selectivity spurred our interest in this compound as a lead for

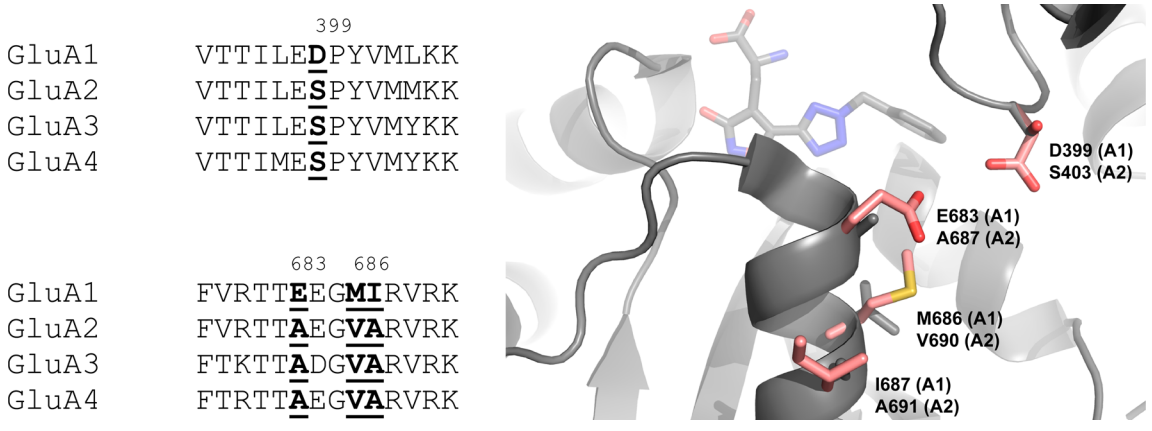

Figure 1. Sequence differences in AMPA receptor agonist binding pockets emphasizing important residues for the pharmacological profile of BnTetAMPA (**5b**). GluA1 residues are displayed in salmon and GluA2 residues in gray. Compound **5b** is shown in stick representation and GluA2 ABD as cartoon (PDB code 2P2A, molB).

DOI: 10.1021/acs.jmedchem.5b01982
J. Med. Chem. XXXX, XXX, XXX−XXX

further medicinal chemistry development. In the present study, we report the design, synthesis, and characterization of a series of BnTetAMPA analogues comprising various modifications to the benzyl group.

RESULTS

Design. In the design of the new compounds, we studied the side pocket to the Glu binding site targeted by the benzyl group of **5b** according to the GluA2 ABD-**5b** crystal structure.[18] A mutation study[19] has suggested that the altered selectivity profile of **5b** compared with **5a** arises from the benzyl group in **5b** protruding into a less conserved region in the AMPA receptor ABD. Four residues in this region are different in GluA1 compared with GluA2−4, and three of these residues were identified as determinants of the subtype selectivity profile of **5b**. Two of the residues are negatively charged acidic residues in GluA1 (Asp399 and Glu683), whereas the corresponding residues in GluA2−4 are neutral residues (Figure 1). We therefore speculated that an amino group protruding from the meta position (**6**) of the benzyl group toward Asp399 and Glu683 would reverse the observed selectivity of **5b**. Furthermore, the opposing meta position was close to a lipophilic area in the binding pocket that potentially could accommodate a chlorine (**7**) or methyl (**8**) group. Along with these analogues, we decided to probe the region further with more variation by introducing CF_3 (**9**) and methylsulfonyl (**10**) groups and by exchanging the benzyl group with a 4-pyridinemethyl group (**11**). Finally, *N*-amino alkylated analogues of **6** (compounds **6a−c**) were also included in the SAR study.

Synthesis. The synthesis of the analogues followed the original procedure,[18] but employing the optimization by Trauner et al.[20] that uses an *O*-allyl protecting group. As shown in Scheme 1, it starts with the tetrazole **12** as a common intermediate for alkylation with 3-substituted benzyl bromides (for **6−10**) or 4-(bromomethyl)pyridine (for **11**) in the presence of potassium carbonate in acetone at room temperature. This gave *N*-2 substituted tetrazoles (**13−19**) as the major regioisomer (the ratio of *N*-1 and *N*-2 regioisomers was varying around 1:4) in high yield. The *N*-1 alkylated regioisomer could not be separated from the *N*-2 alkylated regioisomer at this stage. Various conditions were tested for deprotection of the alkylated tetrazoles, and hydrogen chloride was found to enable removal of all three protecting groups in one step without affecting the *N*-benzyl group. Subsequent purification by reverse phase HPLC gave the final compound as a mixture of the 1- and 2-isomers, which were assigned based on a comparison of NMR signals in accordance with previously reported values. In the case of **6** and **8**, we were able to obtain small amounts of the 1-isomer ((*N*-1)-**6** and (*N*-1)-**8**).

Pharmacology. Initially, all compounds were screened in HEK293 cell lines stably expressing the rat GluA1, GluA2, GluA3, and GluA4 receptors in the Fluo-4/Ca^{2+} assay (see Supporting Information Table S1). In this assay, compound **6** displayed significant agonist activity at GluA1 at concentrations of 30 μM and higher (a complete concentration−response curve could not be generated). In contrast, **6** exhibited no significant activity at the other three subtypes at concentrations up to 1 mM. This interesting profile prompted the synthesis of the *N*-alkylated analogues (**6a−c**) that also exhibited agonist activity in the GluA1-HEK293 cell line in the Fluo-4/Ca^{2+} assay, although the three analogues were observed to be significantly weaker agonists at GluA1 than **6**. Furthermore, **7**

Scheme 1[a]

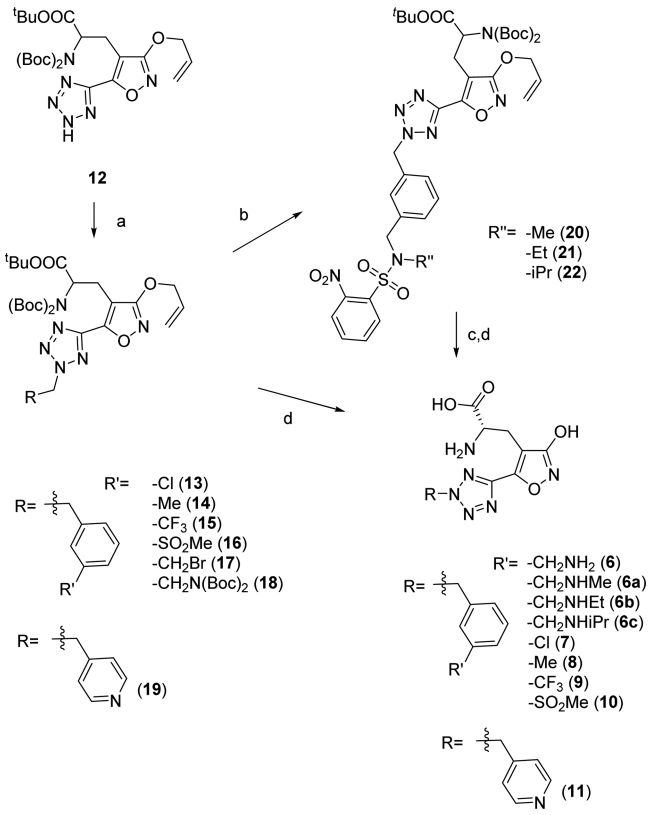

[a]Reagents and conditions: (a) $BrCH_2Ar$, K_2CO_3, acetone, rt; (b) from **17**, *N*-methyl-2-nitrobenzenesulfonamide, K_2CO_3, acetone, rt; (c) PhSH, K_2CO_3, DMF; (d) HCl (37% aq), 90 °C.

displayed agonist activity for all four subtypes, whereas **8** displayed weak antagonism of the Glu-induced response for all of the receptors. All other analogues did not display measurable agonist or antagonist activity at any of the four receptors.

Compounds **6−9** and **11** were selected for characterization of their AMPA, KA, and NMDA receptor binding affinity in a radioligand displacement assay using membranes prepared from rat cortical brain tissue (Table 1). Only **6**, **7**, and **8** showed weak affinity in the AMPA assay compared with compounds **2−5**. The observed affinity for the 1-isomer of **8** ((*N*-1)-**8**) is due to the presence of 3.5% of **8** as determined from NMR and HPLC.

Next we determined the binding affinities of selected compounds to cloned rat AMPA receptor subtypes expressed in *sf9* insect cells (Table 2). Here, the intention with compound **6** to achieve a ligand with inverted selectivity profile compared with **5b** was found to be successful. The affinity of **6** in this assay increased 20-fold at GluA1 compared with **5b**, whereas affinities at other subtypes decreased 4−10-fold. The *N*-alkylated analogues **6a−c** also showed altered selectivity profile although with less pronounced GluA1 preference.

In contrast, the chloro-substituted compound **7** displayed increased binding affinity to all four subtypes compared with **5b**. This was most pronounced at GluA3 where **7** exhibited a 50-fold higher binding affinity than **5b**, thus having a slightly higher affinity to this receptor than AMPA (**2**). At the other three subtypes, the binding affinities of **7** show 3−10-fold increase compared with **5b**. Thus, **7** displayed a significant

DOI: 10.1021/acs.jmedchem.5b01982
J. Med. Chem. XXXX, XXX, XXX−XXX

Table 1. Binding Affinities of Compounds at Native Rat Brain iGluRs

compd	iGluR K_i[f] (μM) AMPA-R	KA-R	NMDA-R
(*RS*)-**2**[a]	0.040	>100	>100
3[a]	0.22	>100	18
4[b]	0.37	>100	>100
(*S*)-**5a**[c]	0.009	11	>100
5b[d]	2.7	>100	87
6	23.1 ± 3.5	>100	>100
6a	>100	>100	>100
6b	>100	>100	>100
6c	>100	>100	>100
6 (*N*-1)	>1000	>100	>100
7	0.80 ± 0.09	>100	>100
8	2.30 ± 0.75	>100	>100
8 (*N*-1)[e]	58 ± 6.3	*g*	*g*
9	>100	>100	*g*
11	>100	>100	>100

[a]Reference 15. [b]Reference 16. [c]Reference 17. [d]Reference 18. [e]Contains 3.5% of the 2-isomer of **8**. [f]Shown are means ± SEM from three to four individual experiments. [g]Not determined.

preference in binding for GluA3 and GluA4 over GluA1 and GluA2 (GluA3 ≈ GluA4 > GluA2 ≈ GluA1). The methyl analogue **8** also displayed increased affinity compared with **5b** at all four subtypes and a similar selectivity profile as **7**. All analogues showed little or no affinity at KA receptor subtypes GluK1−3, which is similar to **5b**. Compound **9** showed little or no affinity at all subtypes tested, whereas **11** was a GluK1 selective ligand. Compound **7** was also characterized on a mutant of $GluA1_o$ where Tyr716 is exchanged for a phenylalanine that is present in the same position in GluA3 and GluA4, resulting in an affinity (K_i = 4.76 μM) that was not statistically significantly different from that at wild-type $GluA1_o$ (*t* test, $p = 0.056$). This observation indicates that this tyrosine/phenylalanine residue is not responsible for increased activity of **7** at GluA3 and GluA4 compared with GluA1 and GluA2 as has been seen with other ligands.[22]

Next we determined the functional properties of the most potent compounds (**6**−**8**) by TEVC electrophysiology at recombinant rat AMPA receptor subtypes expressed in *Xenopus laevis* oocytes (Table 3). In this assay, compound **6** displayed the highest potency (EC_{50} = 19.5 μM) at $GluA1_i$ compared with the other subtypes, although differences were less pronounced compared with the binding affinities (Figure 2A, Table 3). There was no statistically significant difference in the potency of **6** between $GluA1_i$ and $GluA1_o$ ($p > 0.05$, Kruskal−Wallis one-way ANOVA on Ranks), indicating that the flip/flop region of the receptor is not a determining factor for its subtype selectivity. Compounds **7** and **8** displayed some preference for $GluA3_i$ vs $GluA1_i$ ($p < 0.05$, Kruskal−Wallis one-way ANOVA on Ranks with Dunn's post-test). Compounds **6**−**8** showed low efficacy at the cloned AMPA receptor subtypes, indicating that they are partial agonists (Table 3). Compound **7** was a particularly low efficacy agonist at $GluA3_i$ (Figure 2B), suggesting that it might be possible to convert it into a subtype-selective antagonist with some structural modifications.

In order to test our hypothesis that introduction of an electrostatic interaction between the positively charged benzylamino group of **6** and the acidic groups Asp399 and Glu683 in GluA1 was responsible for the inversed selectivity, the compound was characterized pharmacologically at three mutant receptors. We therefore introduced the two acidic residues of $GluA1_i$ into in the corresponding positions of $GluA2(Q)_i$ (Ser403Asp and Ala687Glu). The potencies of Glu at wild-type $GluA2(Q)_i$ and the mutants were not statistically significantly different ($p > 0.05$, Kruskal−Wallis one-way ANOVA on Ranks with Dunn's post-test). Furthermore, the potencies of **6** at wild-type $GluA2(Q)_i$ and the mutants were not statistically significantly different ($p > 0.05$, Kruskal−Wallis one-way ANOVA on Ranks with Dunn's post-test) (Figure 2). However, a trend toward increased relative potency of **6** compared with Glu at GluA2 with introduction of acidic residues can be observed.

Structure. The interesting activity profiles of compounds **6**−**8** spurred us to cocrystallize the compounds with the soluble GluA2 ABD to further understand the binding modes as well as basis of the selectivity of the compounds and their agonist efficacies. The X-ray crystal structures reveal that all three

Table 2. Binding Affinities of Compounds at Cloned Rat iGluR Subtypes Expressed in *sf9* Cells[a]

compd	K_i (μM) $GluA1_o$	$GluA2(R)_o$	$GluA3_o$	$GluA4_o$	GluK1	GluK2	GluK3
2[b]	0.022	0.017[c]	0.021	0.040	1.15	>100	42.7
3[b]	0.13	0.37	27.5	11.9	6.8	>100	90.5
4[c]	0.180	0.348	4.52	13.5	4.48	>100	29.8
(*S*)-**5a**[d]	0.0052	0.0039	0.0022	0.0027	0.081	5.5	>100
5b[e]	7.70	0.75	0.39	0.20	58	39	>100
6	0.434 ± 0.129	8.15 ± 0.92	1.53 ± 0.38	2.75 ± 0.76	16.7 ± 4.8	>100	>100
6a	10.8 ± 3.7	84.4 ± 27.6	8.47 ± 1.21	*h*	>100	>100	>100
6b	5.29 ± 1.30	84.5 ± 28.3	22.3 ± 2.8	*h*	>100	>100	>100
6c	3.2[f]	55[f]	16[f]	*h*	>100	>100	>100
7[g]	0.864 ± 0.060	0.213 ± 0.035	0.00786 ± 0.00126	0.0210 ± 0.0089	1.27 ± 0.21	>100	>100
8	4.61 ± 0.96	1.27 ± 0.35	0.147 ± 0.005	0.522 ± 0.045	6.36 ± 1.34	>100	>100
9	>100	69.1 ± 21.6	4.22 ± 0.96	*h*	*h*	>100	>100
11	>100	>100	19.1 ± 4.6	55.6 ± 4.9	1.05 ± 0.37	>100	>100

[a]Recombinant rat AMPA-R in *sf9* cell membranes. Shown are means ± SEM from $n \geq 3$ experiments conducted in triplicate at 12−16 ligand concentrations. Hill coefficients were close to unity. [b]Reference 15. [c]Reference 16. [d]Reference 17. [e]Reference 18. [f]From one experiment only. [g]K_i at $(Y716F)GluA1_o$ is 4.76 ± 1.46 μM. [h]Not determined

DOI: 10.1021/acs.jmedchem.5b01982
J. Med. Chem. XXXX, XXX, XXX−XXX

Table 3. TEVC Functional Characterization of Compounds 6−8[a]

		6		7		8	
	Glu EC_{50} (μM)	EC_{50} (μM)	efficacy[b]	EC_{50} (μM)	efficacy[b]	EC_{50} (μM)	efficacy[b]
$GluA1_i$	12.5 ± 1.4	19.5 ± 5.0	0.729 ± 0.019	25.7 ± 9.1	0.207 ± 0.012	61.5 ± 8.3	[c]
$GluA1_o$	3.4 ± 0.6	25.1 ± 5.9	[c]	[c]	[c]	[c]	[c]
$GluA2(Q)_i$	14.7 ± 1.4	432 ± 33	[c]	3.66 ± 0.33	0.461 ± 0.020	32.7 ± 2.7	0.346 ± 0.049
$GluA3_i$	21.2 ± 1.4	49.7 ± 11.8	[c]	1.32 ± 0.06	0.0526 ± 0.0105	18.8 ± 2.7	[c]
$GluA4_i$	19.6 ± 2.7	129 ± 34	[c]	4.71 ± 0.58	0.244 ± 0.031	[c]	[c]
$(S403D)GluA2(Q)_i$	13.9 ± 5.4	287 ± 21	[c]	[c]	[c]	[c]	[c]
$(A687E)GluA2(Q)_i$	35.3 ± 4.6	433 ± 40	[c]	[c]	[c]	[c]	[c]
$(S403D,A687E)GluA2(Q)_i$	26.9 ± 4.7	212 ± 27	[c]	[c]	[c]	[c]	[c]

[a]Shown are mean ± SEM ($n \geq 3$ eggs). [b]Efficacy measurements are performed at saturating concentrations of compound in the presence of 100 μM cyclothiazide. Under these conditions, 1 mM (*S*)-Glu is defined to produce an efficacy = 1.000. [c]Not determined.

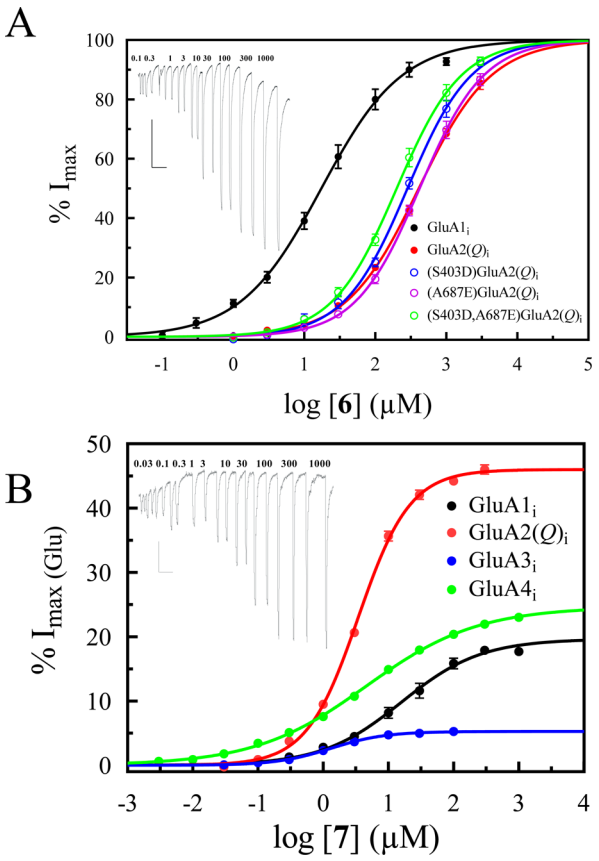

Figure 2. TEVC responses of **6** and **7**. Shown are means ± SEM of normalized, pooled data from 5−9 oocytes. (A) Concentration−response curves of **6** at $GluA1_i$ and wild-type and mutant $GluA2(Q)_i$. Inset shows traces from one $GluA1_i$ expressing oocyte (V_h = −70 mV), conducted in duplicate stimulations at the indicated concentrations (μM) of **6**. Scale bars = 50 nA and 5 min. (B) Concentration−response curves of **7** at $GluA1_i$-4_i scaled to indicate the relative efficacies. Inset shows traces from one $GluA1_i$ expressing oocyte (V_h = −50 mV), conducted in duplicate stimulations at the indicated concentrations (μM) of **7**. Scale bars = 50 nA and 5 min.

compounds bind at GluA2 in a manner very similar to **5b** (see Supporting Information, Figure S1), but with notable differences (Figures 3 and 4).

To accommodate the chlorine in the meta-position of **7**, a displacement of the benzyl group occurs compared with **5b** (Figure 4A), resulting in a lobe 2 movement relative to lobe 1 away from the ligands. A two-dimensional order parameter (ξ1, ξ2) has been introduced to describe the large-scale conformational transitions of the GluA2 ABD.[23] The lobe 2 movement induced by **7** is reflected in a larger ξ2 (defined as the distance between the center of masses of residues 401−403 in lobe 1 and 686−687 in lobe 2), being 8.9 ± 0.2 Å (A 9.1 Å, B 8.9 Å, C 8.7 Å, D 8.9 Å) and 8.3 Å in the structure with **7** and **5b**, respectively (Figure 5). Negligible differences are seen in ξ1 (9.4−9.6 Å; defined as the distance between the center of masses of residues 479−481 in lobe 1 and residues 654−655 in lobe 2). The chlorine atom is accommodated in a cavity created by Tyr405, Thr707, Tyr711, and Trp767 (Figure 4A). Likewise, the benzyl group of **8** is oriented with the methyl group protruding into the same cavity (Figure 4A).

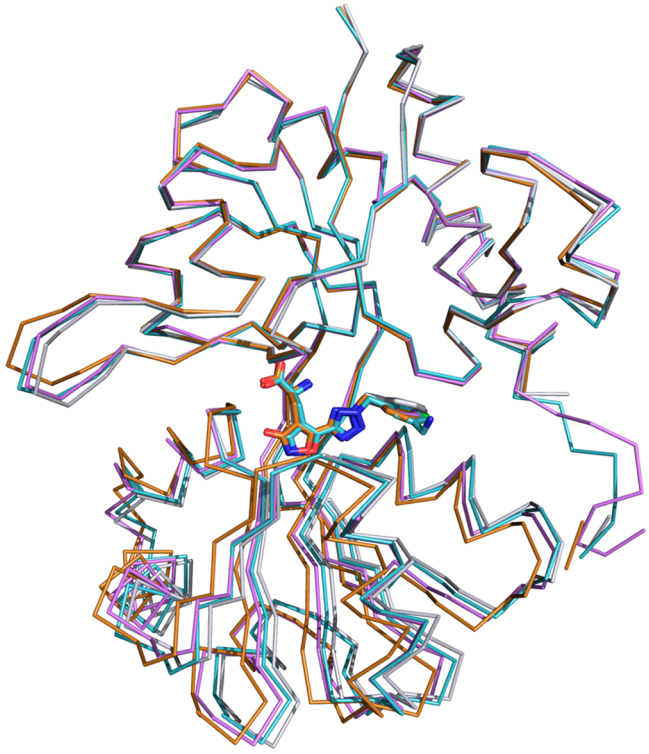

Figure 3. Overlay of X-ray crystal structures of GluA2 ABD with **5b**, **6**, **7**, and **8**. The structures are shown in ribbon representation and overlaid on lobe 1 residues (top). Differences in lobe 2 (lower) movement relative to lobe 1 are seen. **5b**, gray (PDB code 2P2A, molB), **6**, light blue, **7**, orange, and **8**, light purple.

For compound **6**, the benzyl group containing a *meta*-aminomethyl group is flipped in comparison to **5b**, **7**, and **8** in order to enable the amino group to make a salt bridge with Glu402 and a charge-assisted hydrogen bond with Ser403 as

DOI: 10.1021/acs.jmedchem.5b01982
J. Med. Chem. XXXX, XXX, XXX−XXX

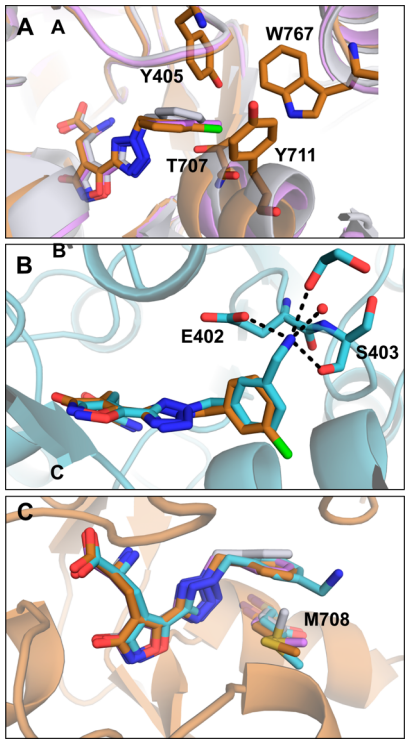

Figure 4. Zoom on ligand binding site of the GluA2 ABD. (A) Comparison of binding mode of **5b**, **7**, and **8**. Residues forming the cavity accommodating the chlorine and methyl group are shown in stick representation. (B) Hydrogen bonding interactions of the aminomethyl group of **6** with GluA2 residues as well as one water molecule and a putative ethylene glycol. The benzyl ring is flipped compared with that in **7**. (C) The conformation of Met708 undergoes induced fit to accommodate the ligands. Color coding as in Figure 3 has been used.

well as contacts to a putative ethylene glycol and a water molecule (Figure 4B). Thereby, the aminomethyl group is interfering with the important interlobe contact between Glu402 and Thr686.[24]

Finally, the side chain conformation of Met708 is affected by binding of the ligands. Met708 has previously been shown to undergo induced fit upon binding of ligands.[25] Whereas Met708 in the structure of **5b** moves away from the binding site compared with other agonist structures like that of **5a**, Met708 is pushed even further in the structures of **6**, **7**, and **8** (Figure 4C).

DISCUSSION AND CONCLUSIONS

In the present study, we present the design, synthesis, and characterization of a series of analogues of the AMPA receptor agonist BnTetAMPA **5b** where variation in the benzyl moiety is introduced. Compound **5b** was developed from the most potent AMPA receptor agonist reported, MeTetAMPA **5a**, and displays a quite unusual activity profile with lower affinity and agonist potency at GluA1 compared with GluA2−4.[17,18] Previously, a few agonists had been developed that discriminated GluA1/GluA2 from GluA3/GluA4 due to the only nonconserved residue (Tyr/Phe) in the Glu binding site of the AMPA receptors,[15,22,26] but the selectivity profile of **5b** (Table 2) could not be explained by this difference. However, the GluA2 ABD crystal structure with **5b**[18] and a modeling study suggested that the benzyl group of **5b** induced movement of Met708 in GluA2 into a nonconserved region of the receptor, where several residues were unique for GluA1.[19] A subsequent mutation study substantiated this hypothesis, since the activity of **5b** at GluA2 could be established in the GluA1 triple mutant Asp399Ser/Met686Val/Ile687Ala.[19] This part of the receptor is generally less conserved in the AMPA receptor subtypes compared with the Glu binding pocket, and this might enable the development of ligands with preference for a single AMPA receptor subtype. We speculate that further variation in moieties of AMPA receptor agonists protruding into this part of the receptor could change the pharmacological profile at the AMPA receptor subtypes and perhaps lead to compounds with preference for individual subtypes.

Introduction of an amino methyl group on the benzyl group (**6**) potentially might favorably interact with two acidic residues (Asp399 and Glu683) in GluA1. Indeed, the affinity at GluA1 increases 18-fold compared with **5b** whereas its affinity at GluA2−4 is decreased 4−14-fold compared with **5b**. Thus, **6** exhibits 3.5-, 6.3-, and 19-fold higher binding affinity at GluA1 than at GluA3, GluA4, and GluA2, respectively. A similar selectivity profile is observed in the TEVC recordings, where **6** displays 2.5-, 6.6-, and 22-fold higher agonist potency at GluA1 than at GluA3, GluA4, and GluA2. This makes **6** the first agonist capable of discriminating between GluA1 and GluA2 both in binding and in functional assays. We therefore probed whether an increased activity of **6** would be observed at GluA2 mutants containing the two acidic amino acids of GluA1 (Asp399 and Glu683 in GluA1; Ser403Asp and Ala687Glu in GluA2). However, there was not any significant change in the potency of **6** at these mutants (nor at the double mutant)

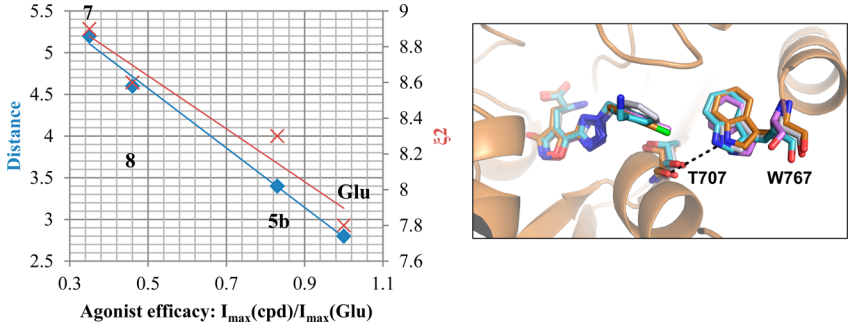

Figure 5. Agonist efficacy of glutamate, **5b**, **7**, and **8**, correlation with the distance in Å (blue) between the indole-*N* of Trp767 and backbone carbonyl oxygen of Thr707 in GluA2, and correlation with distance between the center of masses of residues 401−403 in lobe 1 and 686−687 in lobe 2 (ξ2, red).

DOI: 10.1021/acs.jmedchem.5b01982
J. Med. Chem. XXXX, XXX, XXX−XXX

compared with wild-type GluA2, and probably other residues are involved in the observed selectivity of **6**.

In order to increase the general affinity of the ligands, we introduced chlorine or a methyl group in the meta position of the benzyl group of **5b** that would possibly point into a lipophilic cavity in GluA2. The binding affinity profile of the methyl substituted **8** was very similar to **5b**, but introduction of chlorine yielding **7** led to a 50-fold increase in affinity at GluA3 and only 3−10-fold increases at the other three subtypes. The racemate of **7** is more potent than (*RS*)-AMPA at GluA3 and close to equipotent with the most potent AMPA receptor agonist **5a** assuming that the *R*-form and *N*-1 isomer of **7** is inactive. This assumption is supported by the fact that the *N*-1 regioisomers of **5a**,[17,19] **5b**,[18] **6**, and **8** did not show any significant binding affinity and that the agonist binding domain crystallized from the mixture only with the *N*-1 isomer with (*S*)-configuration in this compound class. We speculated whether the weak affinity of **7** at GluA1 was partly due to Tyr716 in the Glu binding pocket, which corresponds to Phe728 in GluA3 and has been shown to be the determinant for the affinity difference between GluA1/2 and GluA3/4 of **3** and **4**. However, the affinity of **7** at (Tyr716Phe)GluA1$_o$ was unchanged from wild-type, indicating that the selectivity likely comes from the region around the benzyl group and not the bioisosteric isoxazolyl group.

The X-ray structures of the GluA2 ABD with **6**, **7**, and **8** show that the clamshell-like structure is tightly closed around the ligand. It is notable how much the conformation of Trp767 is affected by the chlorine and methyl substituent that seem to push lobe 2 and thus Trp767 away. The degree of receptor activation has been linked to the degree of domain closure based upon the notion that partial agonists induce partial domain closure and that there is a correlation between the degree of domain closure and agonist efficacy as seen in a series of halogen substituted willardiines with varying agonist efficacy.[10,11] This would suggest that the partial domain closure partially shifts the equilibrium between the closed and open channel compared with full agonists. However, an NMR study[12] of the same willardiines showed that a range of dynamic changes was observed that are not visible in the X-ray crystal structures. In particular, the indole N−H signal from Trp767 showed large variation in the NMR study. The rate of HD exchange for the indole N−H of Trp767 is much more rapid when full agonists are bound than when partial agonists are bound. A correlation between large-scale conformational transitions of the GluA2 ABD expressed by the parameter $\xi 2$ (see Results for definition) and the agonist can be seen (Figure 5). However, it is also interesting to note in the X-ray crystal structures of **5b**, **7**, and **8** that the interaction between the indole nitrogen of Trp767 and the carbonyl oxygen of Thr707 shows variation. Thus, a linear correlation can also be seen between the agonist efficacy and the distance between the indole nitrogen in Trp767 and backbone carbonyl oxygen of Thr707 in the structures of Glu, **5b**, **7**, and **8** (Figure 5). Thus, Trp767 might be an important determinant for the agonist efficacy of **5b** analogues. Trp767 is part of helix K that has a disulfide bridge at Cys773−Cys718, so movements in this part can be coupled to other regions. Recent full-length structures with partial agonists[7,8] have provided more insight into the domain movements that might occur upon receptor activation; however, the channel is closed and does not represent a conducting state conformation. One study[7] suggests Ile633 in GluA2 to be an important switch by forming interactions with Ile504, Leu639, Ile645, and Val723. The position of Val723 is close to the disulfide bridge, and it is therefore easy to imagine that changes in the dynamics of helix K could translate to this region. Furthermore, helix K is also linked directly to TM4 and thus could affect ion channel function.

In conclusion, this study shows that the pharmacological activity of ligands at AMPA receptors responds to small changes in the region around the benzyl group of **5b** and that various AMPA receptor subtypes respond differently to these changes. We find that subtle substitutions to the benzyl of **5b** dramatically change the selectivity profile of the compounds and present two novel ligands with interesting selectivity profiles. Compound **6** is the first published agonist capable of discriminating between GluA1 and GluA2 with preference for GluA1, and compound **7** exhibits pronounced selectivity for GluA3 and GluA4 in binding. Changes in both potency and agonist efficacy are observed, and X-ray crystal structures suggest that the agonist efficacy is determined by the bulk introduced at Trp767, whereas residues surrounding the substituted benzyl group determine selectivity. In this sense, the compounds can be important tools for understanding receptor activation mechanisms. Examination of the residues in vicinity of the benzyl group shows that several of them are nonconserved residues, and these differences might be exploited even further. We believe that the biostructural information presented is important for future design of subtype selective AMPA receptor ligands with control of the intrinsic activity. It is currently unknown whether the TetAMPA scaffold is unique or other Glu analogues carrying substituents that can interact with the region around the benzyl group can show similar variation in the pharmacological profile over the AMPA scaffold. Nevertheless, we have clearly demonstrated that the pharmacological profile is highly influenced by subtle changes in this region.

EXPERIMENTAL SECTION

Chemistry. *General Procedures.* All reactions requiring inert conditions were performed in flame-dried glassware under an inert atmosphere of N_2 using standard Schlenk and syringe-septum technique. Petroleum ether (PE, 40−65 °C) was obtained in technical grade and used without further purification. Tetrahydrofuran (THF) was dried using a glass contour solvent system (SG Water, USA LCC). All other solvents for reaction, extraction, and purification were purchased in HPLC grade and used as received. Normal phase column chromatography was performed on silica gel 60 (Merck, 0.015−0.040 mm). Reactions and chromatography fractions were monitored by analytical thin layer chromatography (TLC), which was carried out using silica gel 60 F_{254} aluminum plates (Merck), and the compounds were visualized by using UV light (254 or 365 nm or both) or by spraying with diluted solutions of $KMnO_4$ or ninhydrin. *n*-Butyllithium (*n*-BuLi) was titrated using *N*-pivaloyl-*o*-toluidine prior to use. Intermediate *tert*-butyl 3-(3-(allyloxy)-5-(2*H*-tetrazol-5-yl)isoxazol-4-yl)-2-(bis(*tert*-butoxycarbonyl)amino)propanoate (**S5**) was synthesized according to the published procedures, and the analytical data matched those reported previously.[21] All other starting materials as well as the reagents were obtained from commercial sources and used without further purification. Proton (^{1}H) and carbon (^{13}C) NMR spectra were recorded at 300 K in the solvent indicated. Bruker 400 and Bruker 600 spectrometers were operated at 400 and 600 MHz for proton and at 100 and 150 MHz for carbon nuclei. Chemical shifts (δ) are given in parts per million (ppm) using signals of residual nondeuterated solvent as internal standards. The following abbreviations are used for the proton spectra multiplicities: s, singlet; d, doublet; t, triplet; q, quartet; m, multiplet; br, broad. Coupling constants (J) are given in hertz. For regioisomeric mixtures, fractions of protons are reported for integrals to illustrate the ratio of isomers.

DOI: 10.1021/acs.jmedchem.5b01982
J. Med. Chem. XXXX, XXX, XXX−XXX

LC/MS was performed on an Agilent 1200 system with a Zorbax Eclipse XBD-C18 column (4.6 mm × 50 mm) and UV detector using a linear gradient of the binary solvent system of H_2O/MeCN/formic acid (A = 95/5/0.1 and B = 5/95/0.1) with a flow rate of 1 mL/min (0−90% B over 4 min, then 0.5 min 100% B) equipped with an API ion source (HP 1100 MSD).

Analytical HPLC was performed on a system consisting of an Ultimate 3000 pump and PDA detector, and a TSP AS-3000 autosampler with a Gemini-NX C_{18} column (4.6 mm × 250 mm) or on an Agilent 1260 system with Innoval C_{18} column (4.6 mm × 250 mm) equipped with a 254 nm UV detector using a linear gradient elution of the binary solvent system of H_2O/MeCN/TFA (v/v/v; A = 95/5/0.1 and B = 5/95/0.1) with the concentration of B from 0% to 100% over 20 min with a flow rate of 1.0 mL/min. Preparative HPLC for the purification of final compounds was performed on an Ultimate 3000 system with a Gemini-NX C_{18} column (21 mm × 250 mm) or on a Waters instrument with an Innoval C_{18} column (21.2 mm × 250 mm) equipped with a 254 nm UV detector with the same binary solvent system with a flow rate of 20 mL/min. Purities of the tested compounds were determined by analytical HPLC to be >95%.

Representative synthetic procedures for a few of the compounds are provided.

*(RS)-2-Amino-3-(5-(2-(3-(aminomethyl)benzyl)-2H-tetrazol-5-yl)-3-hydroxyisoxazol-4-yl)propanoic Acid (**6**).* Hydrochloric acid (10 mL, 10 M) was added to **18** (180 mg, 0.21 mmol), and the resulting suspension was stirred for 40 min at 90 °C as the mixture turned clear. The solution was cooled, concentrated, and re-evaporated with water (5 mL × 3). Purification by reverse phase HPLC gave the pure *N*-2-alkylated isomer of **6** (41 mg, 54%) as a white solid. A small amount of pure *N*-1 isomer was also isolated. ^{1}H NMR (400 MHz, D_2O) δ 7.52−7.38 (m, 4.0H), 5.97 (s, 2.0H), 4.19 (dd, J = 7.3, 6.1 Hz, 1.0H), 4.14 (s, 2.0H), 3.34 (dd, J = 15.3, 6.2 Hz, 1.0H), 3.26 (dd, J = 15.3, 7.3 Hz, 1.0H). ^{13}C NMR (101 MHz, D_2O) δ 171.66, 169.85, 155.59, 155.28, 133.59, 133.54, 129.99, 129.64, 129.53, 129.17, 105.44, 56.98, 52.66, 42.75, 22.49. LC/MS (API) Calcd. for $C_{15}H_{17}N_7O_4$: 359.1. Found: 360.1 $[M + H]^+$.

*(RS)-2-Amino-3-(5-(2-(3-chlorobenzyl)-2H-tetrazol-5-yl)-3-hydroxyisoxazol-4-yl)propanoic Acid (**7**).* Hydrochloric acid (10 mL, 10 M) was added to **13** (150 mg, 0.23 mmol), and the resulting suspension was stirred for 40 min at 90 °C as the mixture turned clear. The solution was cooled, concentrated, and re-evaporated with water (5 mL × 3). Purification by reverse phase HPLC gave **7** (50 mg, 60%) as a white solid. The *N*-1 and *N*-2 alkylated isomers could not be separated completely, ^{1}H NMR showed the ratio of the two isomers was 1:3. ^{1}H NMR (600 MHz, DMSO-d_6; 1:3 mixture of regio-isomers) δ 7.46 (s, 1.0H), 7.43−7.26 (m, 4.1H), 7.15−7.11 (m, 0.4H), 6.00 (d, J = 2.3 Hz, 2.1H), 5.83 (s, 0.7H), 3.67 (ddd, J = 9.3, 6.9, 3.9 Hz, 1.5H), 3.25−3.19 (m, 1.5H), 3.00 (dd, J = 16.0, 7.2 Hz, 1.5H). ^{13}C NMR (151 MHz, DMSO-d_6; 1:3 mixture of regio-isomers) δ 172.75, 172.12, 171.65, 171.45, 156.47, 153.69, 150.59, 145.39, 137.17, 136.39, 133.84, 133.80, 131.33, 131.25, 129.25, 128.92, 128.30, 127.74, 126.99, 111.37, 108.26, 55.98, 52.93, 52.64, 51.63, 40.54, 40.40, 39.91, 39.77, 24.87, 24.62. LC/MS (API) Calcd for $C_{14}H_{13}ClN_6O_4$: 364.1. Found: 365.0 $[M + H]^+$.

*(RS)-2-Amino-3-(3-hydroxy-5-(2-(3-methylbenzyl)-2H-tetrazol-5-yl)isoxazol-4-yl)propanoic Acid (**8**).* Hydrochloric acid (10 mL, 10 M) was added to **14** (140 mg, 0.22 mmol), and the resulting suspension was stirred for 40 min at 90 °C as the mixture turned clear. The solution was cooled, concentrated, and re-evaporated with water (5 mL × 3). Purification by reverse phase HPLC gave **8** (21 mg, 28%) as white solid. The *N*-1 and *N*-2 alkylated isomers could not be separated completely; ^{1}H NMR showed the ratio of the two isomers was 1:3.6. ^{1}H NMR (600 MHz, D_2O; 1:3.6 mixture of regio-isomers) δ 7.20 (dd, J = 13.6, 6.2 Hz, 2.2H), 7.14 (t, J = 6.4 Hz, 2.0H), 7.08 (m, 0.5H), 7.03 (s, 0.3H), 6.99 (m, 0.5H), 5.82 (s, 2.0H), 5.79 (s, 0.6H), 4.24 (t, J = 7.0 Hz, 1.4H), 3.32 (dd, J = 15.2, 6.7 Hz, 1.4H), 3.22 (dd, J = 15.2, 7.3 Hz, 1.4H), 2.19 (s, 3.0H), 2.15 (s, 0.8H). ^{13}C NMR (151 MHz, D_2O; 1:3.6 mixture of regio-isomers) δ 176.50, 173.56, 156.15, 153.70, 139.50, 132.93, 129.86, 129.18, 129.13, 125.66, 109.26, 57.18, 54.41, 23.73, 20.34. LC/MS (API) Calcd for $C_{15}H_{16}N_6O_4$: 344.1. Found: 345.1 $[M + H]^+$.

In Vitro Pharmacology. *Native Receptor Binding Assays.* Affinities for native AMPA, KA, and NMDA receptors in rat cortical synaptosomes were determined using 5 nM [^{3}H]AMPA (55.5 Ci/mmol),[27] 5 nM [^{3}H]KA (58.0 Ci/mmol),[28] and 2 nM [^{3}H]CGP 39653 (47.3 Ci/mmol),[29] respectively, with minor modifications as previously described.[30] Rat brain membrane preparations used in these receptor binding experiments were prepared according to a method previously described.[31]

Recombinant Receptor Binding Assays. *Sf9* cells were cultured and infected with recombinant baculovirus of rat AMPA receptors (GluA1$_o$−4$_o$) or rat KA receptors (GluK1−3), and membranes were prepared and used for binding as previously detailed.[17,32] The affinities of the compounds for GluA1$_o$, GluA2(R)$_o$, GluA3$_o$, and GluA4$_o$ were determined from competition experiments with 2−5 nM (*RS*)-[^{3}H]AMPA and at GluK1(Q)$_{1b}$, GluK2(V,C,R)$_a$, and GluK3$_a$ using 5−10 nM [^{3}H]KA (47.2 Ci/mmol). Italic letters in parentheses indicate the RNA-edited isoforms of the subunits. Mutant receptors are numbered according to their full-length protein sequence. Ligand concentration−response curves were analyzed using GraphPad Prism v6 (Graphpad Software Inc., San Diego, CA) to determine the IC_{50}, n_H, and K_i.

TEVC Pharmacology. Surgical procedures were conducted under the approval of the Danish Ministry of Justice Animal Experiments Inspectorate. Mature female *Xenopus laevis* were anaesthetized using 0.1% ethyl 3-aminobenzoate methanesulfonate (tricaine), and ovaries were surgically removed. The ovarian tissue was dissected and treated with 2 mg/mL collagenase in nominally Ca^{2+}-free Barth's medium (in mM: 88 NaCl, 1 KCl, 0.33 $Ca(NO_3)_2$, 0.41 $CaCl_2$, 0.82 $MgSO_4$, 2.4 $NaHCO_3$, 10 HEPES, pH 7.4) for 2 h at room temperature. On the second day, oocytes were injected with 25−50 nL of ∼1 mg/mL rat GluA2(Q)$_i$ cRNA and incubated in Barth's medium with 0.10 mg/mL gentamicin (Sigma Chemical) and 1% penicillin−streptomycin (Life Technologies, Paisley, UK) at 17 °C. Oocytes were typically used for recordings from 3 to 10 days postinjection and were voltage-clamped with the use of a two-electrode voltage clamp (GeneClamp 500B, Axon Instruments, Union City, CA) with both microelectrodes filled with 3 M KCl. Recordings were made while the oocytes were continuously superfused with frog Ringer's solution (in mM: 115 NaCl, 2 KCl, 1.8 $BaCl_2$, 5 HEPES, pH 7.6). Compounds were dissolved in frog Ringer's solution and added by bath application. Recordings were made at room temperature. Efficacy measurements were made in the presence of 100 μM cyclothiazide in order to block receptor desensitization. To determine the maximum response, oocytes were stimulated with 1 mM (*S*)-glutamate plus 100 μM cyclothiazide. Agonist concentration−response curves were analyzed using GraphPad Prism v6 (Graphpad Software Inc., San Diego, CA) to determine the EC_{50} using a four-parameter logistic equation.

Fluo-4/Ca^{2+} Assay. The functional properties of (*S*)-glutamate and compounds 6−11 were characterized in stable GluA1$_i$-, GluA2Q$_i$-, GluA3$_i$- and GluA4$_i$-HEK293 cell lines in the Fluo-4/Ca^{2+} assay essentially as previously described.[33] The cells were split into poly(D-lysine)-coated black 96-well plates with clear bottom (BD Biosciences, Bedford, MA). The medium was aspirated 16−24 h later, and the cells were incubated in 50 μL of assay buffer [Hanks buffered saline solution (HBSS) containing 20 mM HEPES, 1 mM $CaCl_2$, 1 mM $MgCl_2$, and 2.5 mM probenecid, pH 7.4] supplemented with 6 μM Fluo4/AM (Molecular Probes, Eugene, OR) at 37 °C for 1 h. The buffer was aspirated, the cells were washed with 100 μL of assay buffer, and then 100 μL of assay buffer supplemented with 100 μM cyclothiazide was added to the wells (in the antagonist experiments, this buffer was supplemented with various antagonist concentrations). Then the 96-well plate was assayed in a FlexStation3 benchtop multimode microplate reader (Molecular Devices) measuring emission at 520 nm [in fluorescence units (FU)] caused by excitation at 485 nm a total of 90 s before and after addition of 33 μL of agonist solution (the agonists were dissolved in assay buffer). The experiments were performed in duplicate at least three times for each compound at each cell line.

DOI: 10.1021/acs.jmedchem.5b01982
J. Med. Chem. XXXX, XXX, XXX−XXX

X-ray Structures. *Crystallization.* Rat GluA2 ABD (GluR2-S1S2J[24]), comprising segment S1 residues 392−506, a GT linker, and segment S2 residues 631−776 (numbering without signal peptide), was expressed and purified in the presence of L-aspartate as previously reported.[34,35]

Crystallization experiments were performed by the hanging drop vapor diffusion method using drops containing 1 μL of protein solution plus 1 μL of reservoir solution. The drops were equilibrated against 0.5 mL of reservoir solution. All experiments were setup at 6 °C. For the complex of GluA2 ABD with **6**, 4.6 mg/mL GluA2 ABD and 7.8 mM **6** in buffer containing 10 mM HEPES, 20 mM NaCl, and 1 mM EDTA, pH 7.0, was used to crystallize the complex. The crystal used for data collection was obtained from reservoir solution containing 20% PEG4000, 0.3 M lithium sulfate, and 0.1 M sodium acetate buffer, pH 5.5. For the complex of GluA2 LBD with **7**, 5.2 mg/mL GluA2 ABD and 5.3 mM **7** were used, and the crystal used for data collection was obtained from reservoir solution containing 24.4% PEG4000, 0.1 M ammonium sulfate, and 0.1 M acetate buffer, pH 5.5. For the complex of GluA2 ABD with **8**, 5.2 mg/mL GluA2 ABD and 5.3 mM **8** were used, and the crystal used for data collection was obtained from reservoir solution containing 18% PEG4000, 0.1 M ammonium sulfate, and 0.1 M phosphate−citrate buffer, pH 4.5. Before data collection, the crystals were flash cooled in liquid nitrogen after briefly soaking in reservoir solution with 20% glycerol.

Structure Determination. X-ray diffraction data were collected on beamline I911-3 at MAX-lab, Lund, Sweden.[36] The data were processed with XDS[37] (**6**, **7**) or mosflm[38] (**8**) and scaled using SCALA[39] in CCP4i.[40] All three structures were solved by molecular replacement using PHASER[41] within CCP4i. The structure of GluA2 ABD with **5b** (PDB code 2P2A, molB, protein atoms only)[18] was used as search model. Visual inspection of the structures in COOT[42] revealed unambiguous density corresponding to (*S*)-**6**, (*S*)-**7**, and (*S*)-**8**, respectively. Ligand coordinates were generated in Maestro [Maestro, version 9.2, Schrödinger, LLC, New York, NY, 2011] and fitted into the electron density. Topology and parameter files for the ligands were obtained using eLBOW.[43] The structures were refined in PHENIX.[44] The structure of GluA2 ABD with **6** was refined with isotropic B factors, TLS, and riding hydrogen atoms. The structure of GluA2 ABD with **7** was refined with isotropic B factors and riding hydrogen atoms. The structure of GluA2 ABD with **8** was refined with isotropic B factors, TLS, and riding hydrogen atoms. The structures were validated using tools in COOT and PHENIX, as well as the PDB ADIT validation server. Figures were prepared using PyMOL (Schrödinger, LLC, New York, NY). Statistics of data collection and refinement can be found in Supporting Information Table S2.

■ ASSOCIATED CONTENT

Supporting Information

The Supporting Information is available free of charge on the ACS Publications website at DOI: 10.1021/acs.jmedchem.5b01982.

Synthetic procedures for compounds 9−22, pharmacological data from Fluo-4/Ca^{2+} assay (Table S1), crystal data, data collection, and refinement statistics of GluA2 ABD with **6**, **7**, and **8** (Table S2), and electron density and hydrogen bonding interactions for **6**, **7**, and **8** (Figure S1) (PDF)

SMILES compound representations with activity data (CSV)

Accession Codes

The structure coordinates and corresponding structure factor file of GluA2 ABD with **6**, **7**, and **8** have been deposited in the Protein Data Bank under the accession codes 5FHM, 5FHO, and 5FHN, respectively.

■ AUTHOR INFORMATION

Corresponding Authors

*Rasmus P. Clausen, phone +45 35 33 65 66, e-mail rac@sund.ku.dk.

*Darryl Pickering (pharmacology), phone +45 35 33 43 42, e-mail picker@sund.ku.dk.

*Anders A. Jensen (pharmacology), phone +45 39 17 96 50, e-mail aaj@sund.ku.dk.

*Jette S. Kastrup (crystallography), phone +45 35 33 64 86, e-mail jsk@sund.ku.dk.

Notes

The authors declare no competing financial interest.

■ ACKNOWLEDGMENTS

Shuang-Yan Wang was supported by the China Scholarship Council (CSC). A.A.J. was supported by the Novo Nordisk Foundation. Heidi Peterson is thanked for technical assistance with expression and purification of GluA2 ABD. Anne Mette Kærn is thanked for technical assistance with crystallization. The MAX-lab synchrotron facility in Lund, Sweden, is thanked for providing beamtime. The University of Copenhagen Programme of Excellence (GluTarget), the European Community's Seventh Framework Programme (FP7/2007-2013) BioStruct-X under grant agreement no. 283570, and Danscatt are acknowledged for financial support.

■ ABBREVIATIONS

ABD, agonist binding domain; AMPA, (*S*)-2-amino-3-(3-hydroxy-5-methyl-isoxazol-4-yl)propionic acid; MeTetAMPA, 2-amino-3-[3-hydroxy-5-(2-methyl-2*H*-5-tetrazolyl)-4-isoxazolyl]propionic acid; BnTetAMPA, 2-amino-3-[3-hydroxy-5-(2-benzyl-2*H*-5-tetrazolyl)-4-isoxazolyl]propionic acid; Glu, (*S*)-glutamic acid; iGluRs, ionotropic Glu receptors; KA, kainic acid; NMDA, *N*-methyl-D-aspartic acid; TEVC, two-electrode voltage clamp; HEPES, 4-(2-hydroxyethyl)-1-piperazineethanesulfonic acid

■ REFERENCES

(1) Bräuner-Osborne, H.; Egebjerg, J.; Nielsen, E. Ø.; Madsen, U.; Krogsgaard-Larsen, P. Ligands for glutamate receptors: Design and therapeutic prospects. *J. Med. Chem.* **2000**, *43*, 2609−2645.

(2) Dingledine, R.; Borges, K.; Bowie, D.; Traynelis, S. F. The glutamate receptor ion channels. *Pharmacol. Rev.* **1999**, *51*, 7−61.

(3) Traynelis, S. F.; Wollmuth, L. P.; McBain, C. J.; Menniti, F. S.; Vance, K. M.; Ogden, K. K.; Hansen, K. B.; Yuan, H.; Myers, S. J.; Dingledine, R. Glutamate receptor ion channels: structure, regulation, and function. *Pharmacol. Rev.* **2010**, *62*, 405−496.

(4) Sobolevsky, A. I.; Rosconi, M. P.; Gouaux, E. X-ray structure, symmetry and mechanism of an AMPA-subtype glutamate receptor. *Nature* **2009**, *462*, 745−756.

(5) Lee, C.-H.; Lü, W.; Michel, J. C.; Goehring, A.; Du, J.; Song, X.; Gouaux, E. NMDA receptor structures reveal subunit arrangement and pore architecture. *Nature* **2014**, *511*, 191−197.

(6) Karakas, E.; Furukawa, H. Crystal structure of a heterotetrameric NMDA receptor ion channel. *Science* **2014**, *344*, 992−997.

(7) Chen, L.; Dürr, K. L.; Gouaux, E. X-ray structures of AMPA receptor−cone snail toxin complexes illuminate activation mechanism. *Science* **2014**, *345*, 1021−1026.

(8) Yelshanskaya, M. V.; Li, M.; Sobolevsky, A. I. Structure of an agonist-bound ionotropic glutamate receptor. *Science* **2014**, *345*, 1070−1074.

(9) Stawski, P.; Janovjak, H.; Trauner, D. Pharmacology of ionotropic glutamate receptors: A structural perspective. *Bioorg. Med. Chem.* **2010**, *18*, 7759−7772.

DOI: 10.1021/acs.jmedchem.5b01982
J. Med. Chem. XXXX, XXX, XXX−XXX

(10) Jin, R. S.; Banke, T. G.; Mayer, M. L.; Traynelis, S. F.; Gouaux, E. Structural basis for partial agonist action at ionotropic glutamate receptors. *Nat. Neurosci.* **2003**, *6*, 803−810.
(11) Frandsen, A.; Pickering, D. S.; Vestergaard, B.; Kasper, C.; Nielsen, B. B.; Greenwood, J. R.; Campiani, G.; Fattorusso, C.; Gajhede, M.; Schousboe, A.; Kastrup, J. S. Tyr702 is an important determinant of agonist binding and domain closure of the ligand-binding core of GluR2. *Mol. Pharmacol.* **2005**, *67*, 703−713.
(12) Fenwick, M. K.; Oswald, R. E. NMR spectroscopy of the ligand binding core of ionotropic glutamate receptor 2 bound to 5-substituted willardiine partial agonists. *J. Mol. Biol.* **2008**, *378*, 673−685.
(13) Fenwick, M. K.; Oswald, R. E. On the mechanisms of α-amino-3-hydroxy-5-methylisoxazole-4-propionic acid (AMPA) receptor binding to glutamate and kainate. *J. Biol. Chem.* **2010**, *285*, 12334−12343.
(14) Ahmed, A. H.; Ptak, C. P.; Fenwick, M. K.; Hsieh, C.-L.; Weiland, G. A.; Oswald, R. E. Dynamics of cleft closure of the GluA2 ligand-binding domain in the presence of full and partial agonists revealed by hydrogen-deuterium exchange. *J. Biol. Chem.* **2013**, *288*, 27658−27666.
(15) Bjerrum, E. J.; Kristensen, A. S.; Pickering, D. S.; Greenwood, J. R.; Nielsen, B.; Liljefors, T.; Schousboe, A.; Braüner-Osborne, H.; Madsen, U. Design, synthesis, and pharmacology of a highly subtypeselective GluR1/2 agonist, (*RS*)-2-amino-3-(4-chloro-3-hydroxy-5-isoxazolyl)propionic acid (Cl-HIBO). *J. Med. Chem.* **2003**, *46*, 2246−2249.
(16) Frydenvang, K.; Pickering, D. S.; Greenwood, J. R.; Krogsgaard-Larsen, N.; Brehm, L.; Nielsen, B.; Vogensen, S. B.; Hald, H.; Kastrup, J. S.; Krogsgaard-Larsen, P.; Clausen, R. P. Biostructural and pharmacological studies of bicyclic analogues of the 3-isoxazolol glutamate receptor agonist ibotenic acid. *J. Med. Chem.* **2010**, *53*, 8354−8361.
(17) Vogensen, S. B.; Clausen, R. P.; Greenwood, J. R.; Johansen, T. N.; Pickering, D. S.; Nielsen, B.; Ebert, B.; Krogsgaard-Larsen, P. Convergent synthesis and pharmacology of substituted tetrazolyl-2-amino-3-(3-hydroxy-5-methyl-4-isoxazolyl)propionic acid analogues. *J. Med. Chem.* **2005**, *48*, 3438−3442.
(18) Vogensen, S. B.; Frydenvang, K.; Greenwood, J. R.; Postorino, G.; Nielsen, B.; Pickering, D. S.; Ebert, B.; Bølcho, U.; Egebjerg, J.; Gajhede, M.; Kastrup, J. S.; Johansen, T. N.; Clausen, R. P.; Krogsgaard-Larsen, P. A tetrazolyl substituted subtype-selective AMPA receptor agonist. *J. Med. Chem.* **2007**, *50*, 2408−2414.
(19) Jensen, A. A.; Christesen, T.; Bølcho, U.; Greenwood, J. R.; Postorino, G.; Vogensen, S. B.; Johansen, T. N.; Egebjerg, J.; Bräuner-Osborne, H.; Clausen, R. P. Functional characterization of Tet-AMPA [tetrazolyl-2-amino-3-(3-hydroxy-5-methyl-4-isoxazolyl)propionic acid] analogues at ionotropic glutamate receptors GluR1-GluR4. The molecular basis for the functional selectivity profile of 2-Bn-Tet-AMPA. *J. Med. Chem.* **2007**, *50*, 4177−4185.
(20) Stawski, P.; Sumser, M.; Trauner, D. A photochromic agonist of AMPA receptors. *Angew. Chem., Int. Ed.* **2012**, *51*, 5748−5751.
(21) Laprell, L.; Hüll, K.; Stawski, P.; Schön, C.; Michalakis, S.; Biel, M.; Sumser, M. P.; Trauner, D. Restoring light sensitivity in blind retinae using a photochromic AMPA receptor agonist. *ACS Chem. Neurosci.* **2016**, *7*, 15.
(22) Banke, T. G.; Greenwood, J. R.; Christensen, J. K.; Liljefors, T.; Traynelis, S. F.; Schousboe, A.; Pickering, D. S. Identification of amino acid residues in GluR1 responsible for ligand binding and desensitization. *J. Neurosci.* **2001**, *21*, 3052−3062.
(23) Lau, A. Y.; Roux, B. The hidden energetics of ligand binding and activation in a glutamate receptor. *Nat. Struct. Mol. Biol.* **2011**, *18*, 283−287.
(24) Armstrong, N.; Gouaux, E. Mechanisms for activation and antagonism of an AMPA-sensitive glutamate receptor: crystal structures of the GluR2 ligand binding core. *Neuron* **2000**, *28*, 165−181.
(25) Pøhlsgaard, J.; Frydenvang, K.; Madsen, U.; Kastrup, J. S. Lessons from more than 80 structures of the GluA2 ligand-binding domain in complex with agonists, antagonists and allosteric modulators. *Neuropharmacology* **2011**, *60*, 135−50.
(26) Coquelle, T.; Christensen, J. K.; Banke, T. G.; Madsen, U.; Schousboe, A.; Pickering, D. S. Agonist discrimination between AMPA receptor subtypes. *NeuroReport* **2000**, *11*, 2643−2648.
(27) Honore, T.; Nielsen, M. Complex structure of quisqualate-sensitive glutamate receptors in rat cortex. *Neurosci. Lett.* **1985**, *54*, 27−32.
(28) Braitman, D. J.; Coyle, J. T. Inhibition of [^{3}H]kainic acid receptor binding by divalent cations correlates with ion affinity for the calcium channel. *Neuropharmacology* **1987**, *26*, 1247−1251.
(29) Sills, M. A.; Fagg, G.; Pozza, M.; Angst, C.; Brundish, D. E.; Hurt, S. D.; Wilusz, E. J.; Williams, M. [^{3}H]CGP 39653: a new N-methyl-D-aspartate antagonist radioligand with low nanomolar affinity in rat brain. *Eur. J. Pharmacol.* **1991**, *192*, 19−24.
(30) Assaf, Z.; Larsen, A. P.; Venskutonytė, R.; Han, L.; Abrahamsen, B.; Nielsen, B.; Gajhede, M.; Kastrup, J. S.; Jensen, A. A.; Pickering, D. S.; Frydenvang, K.; Gefflaut, T.; Bunch, L. Chemoenzymatic synthesis of new 2,4-syn-functionalized (*S*)-glutamate analogues and structure−activity relationship studies at ionotropic glutamate receptors and excitatory amino acid transporters. *J. Med. Chem.* **2013**, *56*, 1614−1628.
(31) Ransom, R. W.; Stec, N. L. Cooperative modulation of [^{3}H]MK-801 binding to the N-methyl-D-aspartate receptor ion channel complex by L-glutamate, glycine, and polyamines. *J. Neurochem.* **1988**, *51*, 830−836.
(32) Sagot, E.; Pickering, D. S.; Pu, X.; Umberti, M.; Stensbol, T. B.; Nielsen, B.; Chapelet, M.; Bolte, J.; Gefflaut, T.; Bunch, L. Chemoenzymatic synthesis of a series of 2,4-syn-functionalized (*S*)-glutamate analogues: new insight into the structure-activity relation of ionotropic glutamate receptor subtypes 5, 6, and 7. *J. Med. Chem.* **2008**, *51*, 4093−4103.
(33) Strange, M.; Bräuner-Osborne, H.; Jensen, A. A. Functional characterization of homomeric ionotropic glutamate receptors GluR1-GluR6 in a fluorescence-based high throughput screening assay. *Comb. Chem. High Throughput Screening* **2006**, *9*, 147−158.
(34) Juknaitė, L.; Sugamata, Y.; Tokiwa, K.; Ishikawa, Y.; Takamizawa, S.; Eng, A.; Sakai, R.; Pickering, D. S.; Frydenvang, K.; Swanson, G. T.; Kastrup, J. S.; Oikawa, M. Studies on an (*S*)-2-amino-3-(3-hydroxy-5-methyl-4-isoxazolyl)propionic acid (AMPA) receptor antagonist IKM-159: asymmetric synthesis, neuroactivity, and structural characterization. *J. Med. Chem.* **2013**, *56*, 2283−2293.
(35) Krintel, C.; Frydenvang, K.; Ceravalls de Rabassa, A.; Kaern, A. M.; Gajhede, M.; Pickering, D. S.; Kastrup, J. S. L-Asp is a useful tool in the purification of the ionotropic glutamate receptor A2 ligand-binding domain. *FEBS J.* **2014**, *281*, 2422−2430.
(36) Ursby, T.; Unge, J.; Appio, R.; Logan, D. T.; Fredslund, F.; Svensson, C.; Larsson, K.; Labrador, A.; Thunnissen, M. M. The macromolecular crystallography beamline I911−3 at the MAX IV laboratory. *J. Synchrotron Radiat.* **2013**, *20*, 648−653.
(37) Kabsch, W. Integration, scaling, space-group assignment and post-refinement. *Acta Crystallogr., Sect. D: Biol. Crystallogr.* **2010**, *66*, 133−144.
(38) Leslie, A. G. W.; Powell, H. R. Processing diffraction data with mosflm. *Evolving Methods for Macromolecular Crystallography*; Springer: Dordrecht, The Netherlands, 2007; Vol. *245*, pp 41−51.
(39) Evans, P. R. An introduction to data reduction: space-group determination, scaling and intensity statistics. *Acta Crystallogr., Sect. D: Biol. Crystallogr.* **2011**, *67*, 282−292.
(40) Winn, M. D.; Ballard, C. C.; Cowtan, K. D.; Dodson, E. J.; Emsley, P.; Evans, P. R.; Keegan, R. M.; Krissinel, E. B.; Leslie, A. G.; McCoy, A.; McNicholas, S. J.; Murshudov, G. N.; Pannu, N. S.; Potterton, E. A.; Powell, H. R.; Read, R. J.; Vagin, A.; Wilson, K. S. Overview of the CCP4 suite and current developments. *Acta Crystallogr., Sect. D: Biol. Crystallogr.* **2011**, *67*, 235−242.
(41) McCoy, A. J.; Grosse-Kunstleve, R. W.; Adams, P. D.; Winn, M. D.; Storoni, L. C.; Read, R. J. Phaser crystallographic software. *J. Appl. Crystallogr.* **2007**, *40*, 658−674.

DOI: 10.1021/acs.jmedchem.5b01982
J. Med. Chem. XXXX, XXX, XXX−XXX

(42) Emsley, P.; Cowtan, K. Coot: model-building tools for molecular graphics. *Acta Crystallogr., Sect. D: Biol. Crystallogr.* **2004**, *60*, 2126−2132.
(43) Moriarty, N. W.; Grosse-Kunstleve, R. W.; Adams, P. D. electronic Ligand Builder and Optimization Workbench (eLBOW): a tool for ligand coordinate and restraint generation. *Acta Crystallogr., Sect. D: Biol. Crystallogr.* **2009**, *65*, 1074−1080.
(44) Adams, P. D.; Afonine, P. V.; Bunkoczi, G.; Chen, V. B.; Davis, I. W.; Echols, N.; Headd, J. J.; Hung, L. W.; Kapral, G. J.; Grosse-Kunstleve, R. W.; McCoy, A. J.; Moriarty, N. W.; Oeffner, R.; Read, R. J.; Richardson, D. C.; Richardson, J. S.; Terwilliger, T. C.; Zwart, P. H. PHENIX: a comprehensive Python-based system for macromolecular structure solution. *Acta Crystallogr., Sect. D: Biol. Crystallogr.* **2010**, *66*, 213−221.

DOI: 10.1021/acs.jmedchem.5b01982
J. Med. Chem. XXXX, XXX, XXX−XXX